International Journal of Applied Engineering Research ISSN 0973-4562 Volume 10, Number 17 (2015) pp 38090-38095

Grain structure evolution at sintering of the bulk Bi_2Te_3 nanomaterial under hot pseudo-isostatic pressure

Oleg Ivanov, Roman Lyubushkin, and Oxana Soklakova

Belgorod State National Research University,
Joint Research Centre
"Diagnostics of structure and properties of nanomaterials"
Pobedy St., 85, 308015, Belgorod, Russian Federation

Abstract
Bulk nanograined Bi_2Te_3 material with various mean grain size changing from ~ 97 nm to ~ 51 nm was prepared by microwave assisted solvothermal method and hot pseudo-isostatic pressure. The mean grain size values obtained for various pressures, P, and temperatures, T, of the sintering process were used to estimate the changes of activation volume, V^*, for self-diffusion process responsible for grain growth at sintering of material under study. Analysis of the $V^*(P)$ dependences taken at 573 K and 673 K allowed us to suggest that one interstitial mechanism takes place at 573 K, while the diffusion mechanism is assumed to be changed from the vacancy mechanism at low pressures (2 GPa and 4 GPa) to the interstitial mechanism at high pressures (6 GPa and 8 GPa) at 673 K.

Keywords: bulk nanograined materials, grain structure, activation volume of diffusion

Introduction

Thermoelectric materials are of interest for applications in electrical power generation devices and solid-state cooling due to many attractive properties (long life, no emissions of toxic gases, no moving parts, low maintenance, etc.) [1]. It is known [2] that thermoelectric efficiency of materials is characterized by a dimensionless thermoelectric figure-of-merit (ZT), defined as ($S^2\sigma/k$), where Z is the figure-of-merit, T is the absolute temperature, S is the Seebeck coefficient, σ is the electrical conductivity, and k is the total thermal conductivity with contributions from the crystal lattice and the charge carriers. So, it is clear that the materials with high S and σ values, but low k are desirable to achieve good ZT values.

Recent researches [3-6] show that significant ZT enhance can be reached for thermoelectric nanostructures by reducing the thermal conductivity via effective phonon scattering without too much affecting the power factor, $S\sigma^2$. For instance, the bulk nanograined materials are now considered to be ones of perspective thermoelectric materials. High enough electrical conductivity, but low enough lattice thermal conductivity should be for the same time combined for these materials. It is assumed [7] that the ZT value in the bulk nanograined materials can be significantly enhanced by reducing the lattice thermal conductivity via effective phonon scattering, because numerical grain boundaries act as phonon scattering centers.

The bulk nanograined materials are usually produced by nanopowder consolidation by various methods [8]. The key to the nanopowder consolidation process of thermoelectric materials is to minimize to the grain growth during the consolidation, because the grains easily grow to micron-size, which degrades the nano-effects [9]. To preserve nanostructure in the bulk materials, various methods are applied including the spark plasma sintering, pressure-assisted consolidation methods, microwave sintering, field-assisted sintering, etc. One of these methods relating to pressure-assisted consolidation methods is hot pseudo-isostatic pressure (HPIP) method using toroidal-type apparatuses [10]. Pressure levels up to 6-8 GPa can be attained by using HPIP-method. Both high temperature and high pressure simultaneously act on material in HPIP-method. Therefore, the sintering time is significantly reduced and the grain growth can be suppressed.

The aim of this paper is to analyze the grain structure evolution at the HPIP-sintering of the bulk Bi_2Te_3 nanomaterial. At present, bismuth telluride, Bi_2Te_3, based compounds are known to be the best thermoelectric materials for around room temperature applications [11].

2. Material and methods

Microwave-solvothermal synthesis (closed reactor ERTEC model 02-02) was applied to prepare the nanosized Bi_2Te_3 powder. As is known, compared with the conventional methods, the microwave-assisted heating technique has the advantages of very short time of synthesis, simplicity and energy efficiency, small particle size of the products, narrow particle size distribution and high purity [12].

The analytical grade Bi_2O_3, TeO_2 and ethylene glycol were used as starting components. A 110 ml teflon-lined stainless-steel autoclave was used and the temperature was regulated by a digital-type temperature-controlled oven. Microwave assisted reactions were conducted in a 300 W microwave oven with a 2450 kHz working frequency. The ethylene glycol was used as both the solvent and reducing agent in the reaction. After synthesis, the reaction product as a black precipitate was washed with alcohol and then centrifuged and dried.

To sinter the bulk Bi_2Te_3 material, the powders after synthesis were hot pseudo-isostatically pressed by using a toroidal press. The powder for consolidation was placed in a graphite matrix with hexagonal BN powder as a media spreading the pseudo-isostatic pressure to the object under pressing. HPIP-parameters presented in next section of this paper.

X-ray diffraction (XRD) analysis both the powder and bulk material was performed for the phase and crystal structure determination by using a Rigaku Ultima IV diffractometer with CuK_α - radiation (a step width of 0.03° and a counting time of 1.6 s/step).Transmission electron microscope (TEM), JEM – 2100, was applied to study morphology of the powders (for an accelerating voltage of 200 kV).Scanning electron microscope (SEM), Quanta 200 3D, was used to examine the grain structure of the bulk material (for an accelerating voltage of 2 kV).

3. Results and Discussion

To optimize the phase composition of theBi_2Te_3 powders, a few routes of the microwave-solvothermal synthesis were applied (Table 1). According to Table 1, the phase composition of the powders is drastically dependent on synthesis conditions. Only one of synthesis routes allowed us to prepare a single-phase powder of the Bi_2Te_3 composition. The optimal synthesis conditions are as follows: temperature is 523 K, pressure is 15 atm., duration of synthesis is 50 min and ratio of Bi_2O_3 and TeO_2 is 1: 1.

The XRD pattern for the single-phase Bi_2Te_3 powder taken at room temperature is shown in Figure 1.The diffraction peaks can be exactly indexed with the standard diffraction planes of hexagonal Bi_2Te_3 (space symmetry group is $R\bar{3}m$). This powder synthesized at the optimal conditions was used for further examination.

TEM image in Figure 2 shows a typical morphology of the microwave-solvothermally synthesized powder. It is seen that the powder mainly consists of irregularly shaped nanoparticles of 20 - 50 nm in size.

In order to estimate a mean nanoparticle size, histogram of the nanoparticles size distribution was plotted (Figure 3). It was found that the experimental histogram can be described in frames of a unimodal lognormal distribution. It is known [13] that the lognormal probability density function can be written as

$$F(d) = \frac{1}{\sqrt{2\pi}\sigma d}\exp\left(-\frac{(\ln d-\ln d_m)^2}{2\sigma^2}\right), \quad (1)$$

where d is the nanoparticle size, d_m is the mean nanoparticle size and σ is the standard deviation of the logarithms of the nanoparticle sizes.

One can see that expression (1) reproduces the experimental nanoparticle size distributions very well. The d_m value was estimated to be equal to ~ 28 nm.

Hot pseudo-isostatic pressure method was further used to prepare the bulk Bi_2Te_3 material. To examine the grain structure evolution during the HPIP-sintering, the various HPIP-pressures and HPIP-temperatures were applied. The samples were sintered at the HPIP-pressures, P, of 2, 4, 6 and 8 GPa and at the HPIP-temperatures, T, of 573 K and 673 K during 5 min. It was found that both the HPIP-pressure and HPIP-temperature really influence on the grain structure of the material under study. For instance, the SEM images of the surfaces of the samples prepared at the HPIP-pressures of 2, 4, 6 and 8 GPa and at the HPIP-temperature of 573 K are shown in Figure 4.

The materials prepared by HPIP-method have dense, homogeneous and porousless, nanocrystalline structures. Spherical formations with diameters of 150-350 nm are observed for the sample with the HPIP-pressure of 2 GPa (Figure 4 a). Since the nanoparticles size of the microwave-solvothermally synthesized powder was less or equal to 50 nm (Figure 2), the large spherical structures should be considered as agglomerates consisting of a lot of nanoparticles.

Smaller spherical particles can be also seen for this sample. So, the grain structure of the bulk polycrystalline material is not yet formed at 2 GPa. The large spherical agglomerates typical for the HPIP-pressure of 2 GPa are practically absent for other P values (Figure 4 b, c and d).

Only smaller grains mainly with sizes less than 100 nm are now observed on the SEM images. The grains have a crystal faceting that can be taken as evidence of intense sintering of the nanopowder. To characterize the HPIP-pressure and HPIP-temperature effect on the grain structure characteristics in detail, histograms of the grain size distributions for various T and P values were plotted. For instance, Figure 5 shows such histograms for the HPIP-temperature of 673 K and the HPIP-pressures of 2 and 8 GPa. Diameters, D_g, of more than 200 grains were measured on the SEM images (Figure 4) to obtain reliable size distribution. The grain size distributions are discretized by dividing them into the 20 nm - width segments.

The unimodal lognormal distribution was again applied to describe the experimental histograms of the grain size distributions and estimate the mean grain size, D_{gm}. Maximum D_{gm} value equal to 97 nm was found for the HPIP-pressure of 2 GPa and the HPIP-temperature of 573 K, while minimum D_{gm} value equal to 51 nm is corresponding to the HPIP-pressure of 8 GPa and the HPIP-temperature of 673 K The $D_{gm}(P)$ dependences taken for the HPIP-temperatures of 573 K (curve *1*) and 673 K (*2*) are presented in Figure 6. It should be noted that the curves *1* and *2* behave quite differently. The $D_{gm}(P)$ dependence for the HPIP-temperature of 573 K is steady falling as P increases, while a weak maximum in the $D_{gm}(P)$ dependence can be seen for the HPIP-temperature of 673 K.

Usually, the grain growth during the sintering is due to processes of high-temperature atomic self-diffusion of substance under sintering [14]. As for our experiment, pressure effect on diffusion processes should be taken into account in addition to the sintering temperature.

It is known [15] that the diffusion coefficient, D, is dependent on pressure as given by the expression

$$D(P) = D(0)\exp\left(-\frac{PV^*}{RT}\right), \quad (2)$$

where R is the gas constant and V^* is the activation volume. The activation volume is corresponding to the volume expansion of solid related to atomic rearrangements during the thermally activated process based on concrete diffusion mechanism.

It should be noted that knowledge of the V^* value permits to draw conclusions concerning the diffusion mechanism of the process under study. According to Ref. [15], V^* can be obtained from the equation

$$V^* = -RT\frac{ln(v)}{P}, \quad (3)$$

where v is the rate of the process under study.

In order to determine the $v(P)$ dependence at constant temperature for our experiment, the $D_{gm}(P)$ dependences for

the HPIP-temperatures of 573 and 673 K can be used. Indeed, according to Ref. [15], the displacement, l, of a grain boundary during high-temperature annealing under high pressure is

$$l = \upsilon t = t\upsilon_0\left(\frac{Q}{RT}\right)\exp\left(-\frac{PV^*}{RT}\right), \quad (4)$$

where υ is now rate of the grain boundary motion, t is the annealing time, υ_0 is the pre-exponential factor and Q is the activation energy.

This expression can be used to extract the $V^*(P)$ dependence. Let us believe that initial mean grain size is equal to mean nanoparticle size of the Bi_2Te_3 powder before HPIP-sintering. Besides, the shape of grains during the sintering will be assumed to be spherical. Then, the displacement of the grain boundary during the HPIP-sintering can be expressed as

$$l = \frac{D_{gm}-d_m}{2}. \quad (5)$$

The $l(P)$ dependence obtained by using the expression (5) for the HPIP-temperature 573 K is presented in Figure 6, inset. This dependence can be described by expression

$$l = 11.65 + 48.4\exp\left(-\frac{2.68}{P}\right) \quad (6)$$

as is shown by solid line in inset. Here l_0 = 48.4 nm is the l value at P=0 GPa. So, l_0 can be used to estimate the grain growth at sintering without external pressure (at ambient pressure). Now, the mean grain size for HPIP-pressureless sintering can be calculated to be equal to

$$D_{gm}(P=0)=2(l_0+d_m)\approx 125 \text{ nm}. \quad (7)$$

In accordance with way published in Ref. [15], the ratio of the mean square grains, $S(P)/S(0)$, will be used as the v value in the expression (3). The $S(0)$ value was estimated to be equal to $12.2\cdot10^{-15}$ nm^2. The S and v values for various HPIP-temperatures and HPIP-pressures are given in Table 2. Besides, the V^* values calculated by using the expression (3) are also presented in this Table.

The $V^*(P)$ dependences obtained for both HPIP-temperatures are shown in Figure 7. One can see that for the HPIP-temperature of 573 K the activation volume is characterized by a weak P-dependent, while for the HPIP-temperature of 673 K the activation volume firstly decreases and then tends to some saturated value as the HPIP-pressure gradually increases. Such kind of the $V^*(P)$ behaviors allowed us to assume that the diffusion process mechanism changes at the HPIP-pressure increasing for the HPIP-temperature of 673 K. In contrast, the diffusion process for the HPIP-temperature of 573 K is rather characterized by one mechanism for all HPIP-pressures.

Atomic volumes of Te and Bi are equal to $20.44\cdot10^{-6}$м^3□mol and $21.43\cdot10^{-6}$м^3□mol, respectively. These values much bigger than the V^* values extracted from our experimental data. It is known [15] that under $V^* \rightarrow 0$ Ω (character Ω denotes atomic volume) condition an interstitial diffusion mechanism takes place. But a vacancy diffusion mechanism will occur under $V^* \rightarrow 1$ Ω condition. So, by comparing the atomic volumes of Te and Bi with the V^* values (Figure 8), interstitial diffusion mechanism can be assumed as main mechanism for the HPIP-temperature of 573 K. For the HPIP-temperature of 673 K the same interstitial diffusion mechanism can be assumed to be responsible for diffusion process only for high HPIP-pressures of 6 and 8 GPa. At less HPIP-pressures, another diffusion mechanism should be considered. Taking into account a rapid V^* increase at $P \rightarrow 0$ (Figure 7), another diffusion mechanism might be the vacancy mechanism of self-diffusion. So, the change of the diffusion mechanism may occur at the HPIP-sintering the bulk Bi_2Te_3 nanomaterial.

It should be noted that the change of the diffusion mechanism under high pressure have also been considered, for instance, to account for the diffusion process for silver into lead [16].

4. Conclusion

The bulk Bi_2Te_3 nanomaterial with various mean grain size changing from ~ 97 nm to ~ 51 nm was prepared by the microwave assisted solvothermal method and hot pseudo-isostatic pressure. The D_{gm}values obtained for various HPIP-pressures and HPIP-temperatures were used to estimate the changes of the activation volume of self-diffusion process responsible for the grain growth during the sintering the material under study. Analysis of the $V^*(P)$ dependences taken for the HPIP-temperatures of 573 K and 673 K allowed us to suggest that one interstitial mechanism takes place for the HPIP-temperature of 573 K, while the diffusion mechanism is assumed to change from the vacancy mechanism at low HPIP-pressures to the interstitial mechanism at high HPIP-pressures for the HIP-temperature of 673 K.

Acknowledgements

All of studies were carried out by the scientific equipment of the joint research center "Diagnostics of structure and properties of nanomaterials" of Belgorod National Research University what is financially supported with Ministry of Science and Education of RF under project № 14.594.21.0010, unique code RFMEFI59414X0010. This work was also financially supported by the Ministry of Education and Science of the Russian Federation under projects No 2014/420-1.

References

[1] G. Mahan, B. Sales, J. Sharp, Thermoelectric Materials: New Approaches to an Old Problem, Phys. Today, 50 (1997) 42-47.

[2] T.M. Tritt, Holey and unholey semiconductors, Science, 283, (1999) 804-805.

[3] W. Liu, X. Yan, G. Chen, Z. Ren, Recent advances in thermoelectric nanocomposites. NanoEnergyNano Energy, 1 (2012) 42-56.

[4] K. Liu, T. Wang, H. Liu, D. Xiang, Preparation and characterization of nanostructured Bi_2Se_3 and $Sn_{0.5}$-Bi_2Te_3, Rare Metals Rare Metals, 28 (2009) 112-16.

[5] T.C. Harman, M.P. Walsh, B.E. Laforge, G.W. Turner. Nanostructured thermoelectric materials, J. Electr. Mat., 34 (2005) 19-26.

[6] Y.Q. Cao, T.T. Zhu, X.B. Zhao, X.B. Zhang, J.P. Tu. Nanostructuring and improved performance of ternary Bi-Sb-Te thermoelectric materials, Appl. Phys. A, 92, (2008) 321-324.

[7] P. Pichanusakorn, P. Bandaru, Nanostructured thermoelectric Materials Science and Engineering R, 67 (2010) 19-63.
[8] J.R. Groza. Nanostructured Materials, 12 (1999) 987-992.
[9] Qian Zhang, Qinyong Zhang, S. Chen, W. Liu, K. Lukas, X. Yan. H. Wang, D. Wang, C. Opell, G. Chen, Z. Ren., Suppression of grain growth by additive in nanostructured p-type bismuth antimony tellurides, NanoEnergy, 1 (2012)183-189.
[10] L. G. Khvostantsev, V.N. Slesarev, V.V. Brazhki, Toroid type high-pressure device: history and prospects, High Pressure Research, 24 (2004) 371-383.
[11] D.Y. Chung, T. Hogan, P. Brazis, M. Rocci-Lane, C. Kannewurf, M. Bastea. $CsBi_4Te_6$: A High Performance Thermoelectric Material for Low-Temperature Applications, Science, 287 (2000) 1024-1027.
[12] Deng, X.S. Zhou, G.D. Wei, J. Liu, C.W. Nan, S.J. Zhao, Solvothermal preparation and characterization of nanocrystalline Bi_2Te_3 powder with different morphology, J. Phys. Chem. Solids, 63 (2002) 2119-2122.
[13] F.J. Humpreys, M. Hatherly. Recrystallization and Related Annealing Phenomena. Oxford, UK; Elsevier, 2004.
[14] B.J. Buescher, H.M. Gilder, N. Shea, Temperature-dependent activation volumes of self-diffusion in cadmium, Phys. Rev. B, 7 (1973) 2261-2268.
[15] V. Sursaeva, S. Protasova, W. Lojkowski, J. Jun, Microstructure evolution during normal grain growth under high pressure in 2-D aluminium foils, Textures and Microstructures, 32 (1999)175-185.
[16] H.R. Curtin, D.L. Decker, H.B. Vanfleet, Effect on pressure on the intermetallic diffusion on silver in lead, Phys. Rev. B, 139 (1965) A1552-A1557.

Appendix 1. Figures and tables.

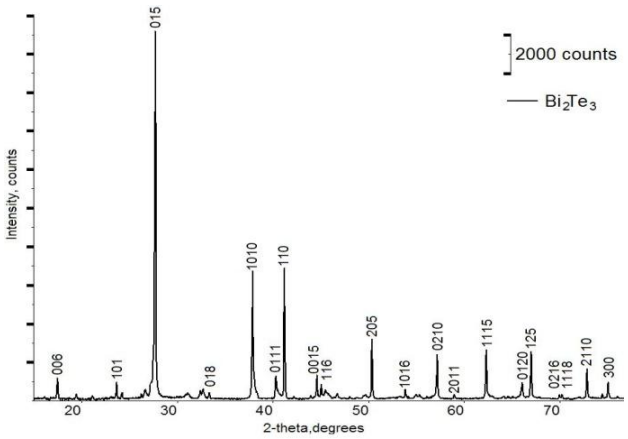

Figure 1. XRD pattern of the Bi_2Te_3 powder.

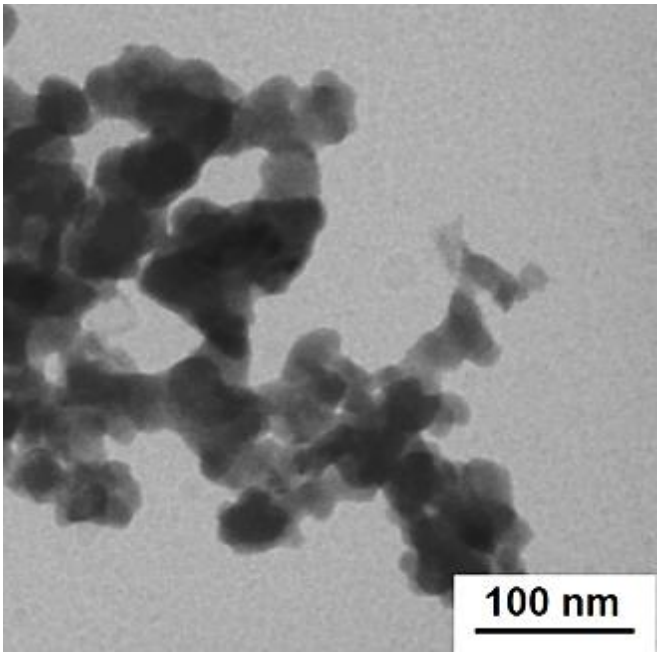

Figure 2. TEM image of the Bi_2Te_3 nanopowder.

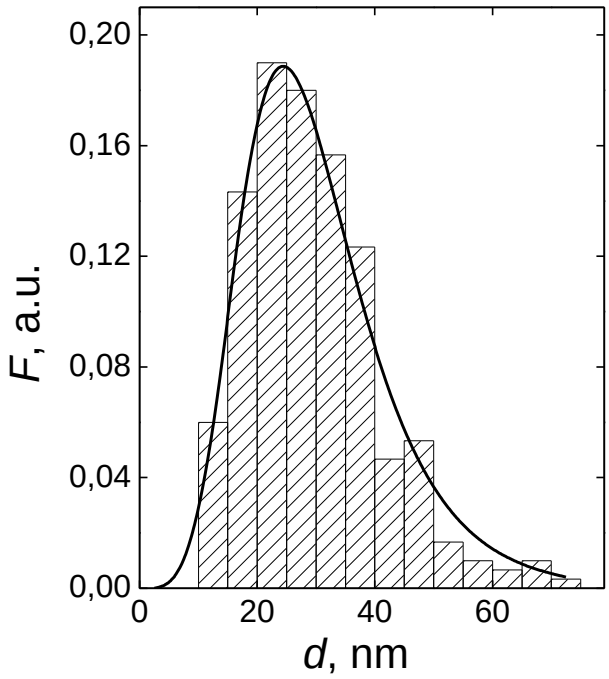

Figure 3. Histogram of the Bi_2Te_3 nanoparticles size distribution.

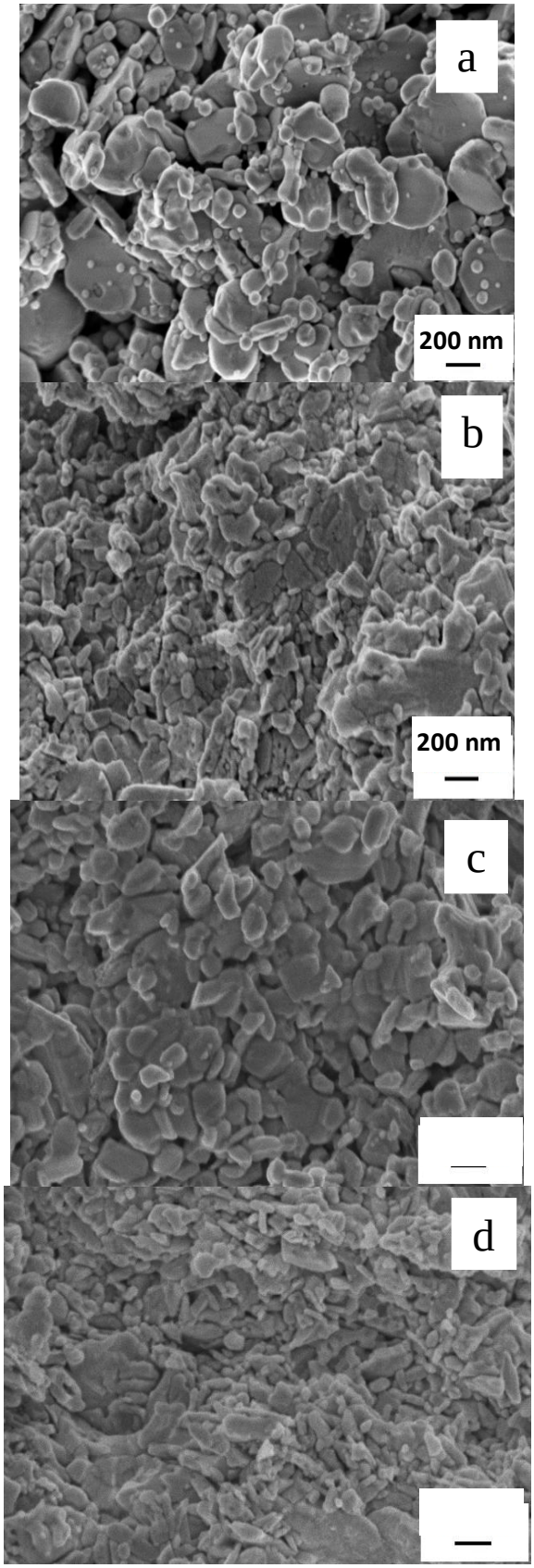

Figure 4. SEM images of the bulk Bi_2Te_3 nanomaterial sintered at the HPIP-temperature of 573 K and various HPIP-pressures: (a) 2, (b) 4, (c) 6 and 8 GPa (d).

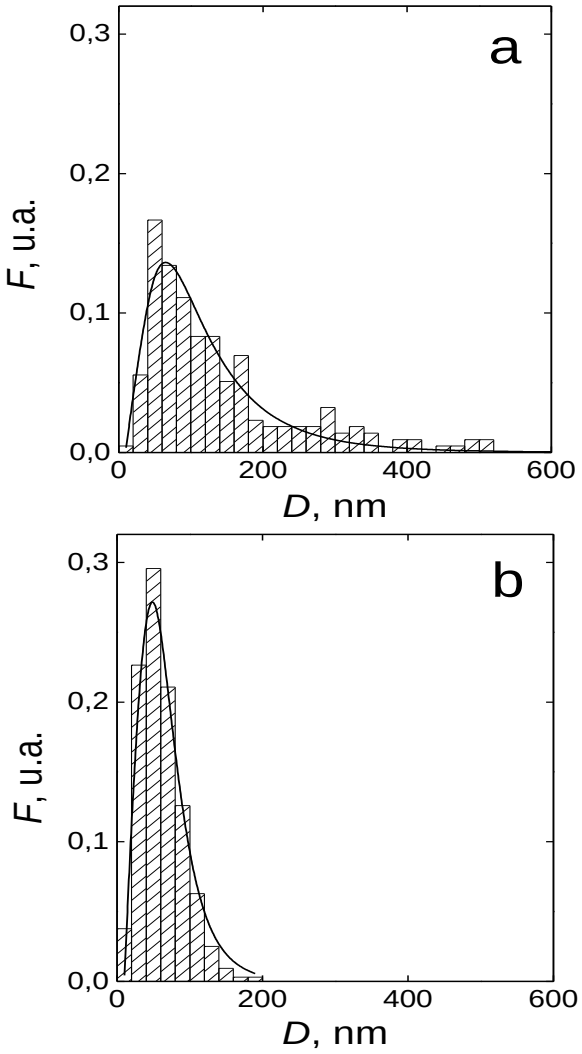

Figure 5. Histograms of the grain size distributions for the bulk Bi_2Te_3 material sintered at the HPIP-temperature of 573 K and various *P* values: 2 (a) and 8 GPa (b). Solid lines are fits to the lognormal distribution.

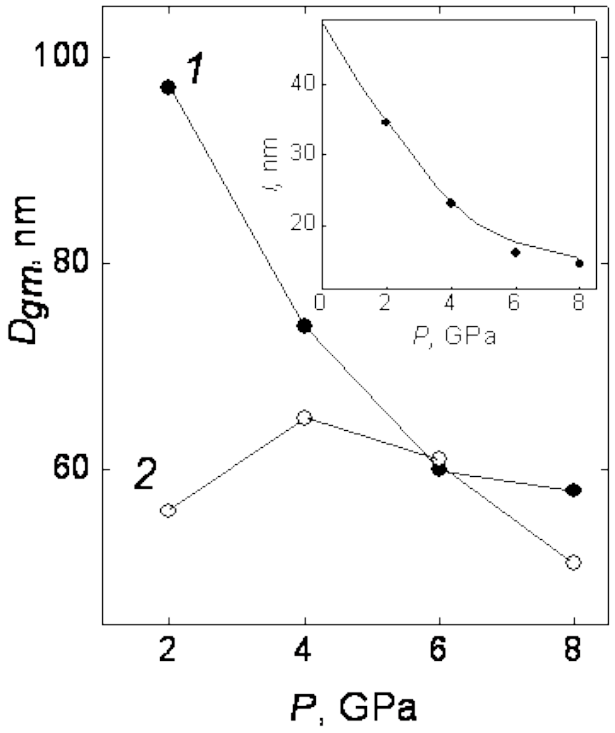

Figure 6. The$D_{gm}(P)$ dependences for the HPIP-temperatures of 573 K (curve *1*) and 673 K (*2*). **The inset is the $l(P)$ dependence.**

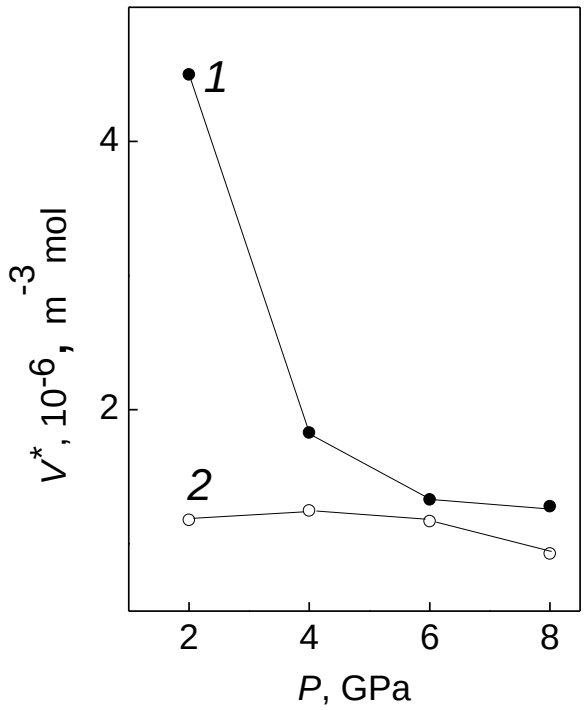

Figure 7. The$V^*(P)$ dependences for the HPIP-temperatures of 573 K (curve *1*) and 673 K (*2*).

Table 1. Parameters and results of the microwave-solvothermal synthesis of the powders.

Reagents	Parameters of synthesis	Phases
Ethylene glycol – 60 ml *m* (Bi_2O_3) - 4.6 g *m* (TeO_2) – 2.3 g	Temperature – 553 K Pressure – 25 atm. Duration of reaction – 100 min.	Bi_2Te_3, Bi, BiTe
Ethylene glycol – 60 ml *m* (Bi_2O_3) - 4.6 g *m* (TeO_2) – 3 g	Temperature – 553 K Pressure – 37 atm. Duration of reaction – 45 min.	Bi_2Te_3, Bi, Te
Ethylene glycol – 60 ml *m* (Bi_2O_3) – 2.3 g *m* (TeO_2) – 1.5 g	Temperature – 523 K Pressure – 30 atm. Duration of reaction – 35min.	Bi_2Te_3, Bi, Bi_4Te_3
Ethylene glycol – 60 ml *m* (Bi_2O_3) – 2.3 g *m* (TeO_2) – 2.3 g	Temperature – 523 K Pressure – 15 atm. Duration of reaction – 50 min.	Bi_2Te_3
Ethylene glycol – 60 ml *m* (Bi_2O_3) – 2.3 g *m* (TeO_2) – 2.45 g	Temperature – 523 K Pressure – 20 atm. Duration of reaction – 35 min.	Bi_2Te_3, Bi_4Te_3

Table 2 Results of analysis of the grain growth at the HPIP-sintering thebulk Bi_2Te_3 nanomaterial.

HPIP-pressure, GPa	S, 10^{-15}, nm^2		v		V^*, 10^{-6}, $м^3$□mol	
	HPIP-temperature, K		HPIP-temperature, K		HPIP-temperature, K	
	573	673	573	673	573	673
2	7.4	2.5	0.61	0.20	1.18	4.5
4	4.3	3.3	0.35	0.27	1.25	1.83
6	2.8	2.9	0.23	0.24	1.17	1.33
8	2.6	2.0	0.21	0.16	0.93	1.28